AIAA SciTech Forum
8–12 January 2018, Kissimmee, Florida
2018 AIAA Aerospace Sciences Meeting

10.2514/6.2018-0038

Unsteady Viscous Lift Frequency Response Using The Triple Deck Theory

Haithem Taha* and Amir Rezaei†
University of California, Irvine, CA 92697

Many reports, studies, and evidences invoke an alternative auxiliary condition to the Kutta condition for the analysis of unsteady flows around wings with sharp edges. Some of these reports, because of the observed discrepancies at zero lift conditions, suggested a fundamental revision to the classical theory of unsteady aerodynamics. That is, since the vorticity generation and lift development are essentially viscous processes, a purely inviscid theory of unsteady aerodynamics might be fundamentally flawed. In this work, an unsteady boundary layer approach (triple deck theory) is adopted to develop a viscous correction to the unsteady lift frequency response; i.e., a Reynolds-number dependent extension of Theodorsen function. The developed model is weakly nonlinear, but so compact and efficient that it may be used in flight dynamics, control, and aeroelastic analyses. It is found that the viscous correction induces a significant phase shift to the circulatory lift component, particularly at low Reynolds numbers and high-frequencies, that matches expectations based on previous experimental results. This enhancement in the predicted phase of the unsteady loads is envisaged to boost the current predictability of aeroelastic flutter boundaries. High-fidelity computational fluid dynamic simulations are also carried out to validate the results of the developed theoretical model.

I. Introduction

Most of the last century analytical developments of unsteady aerodynamics of wings in an incompressible flow were based on Prandtl's concept (vortices form behind the airfoil whose strength and shape are not specified apriori[1]). Moreover, for infinitely thin airfoils, separation or sheets of vorticity are shed from the sharp edges only and the flow outside of these sheets can be modeled using inviscid assumptions.[2] These concepts, in addition to assuming small disturbance to the mean flow (flat wake assumption), form the heart of the classical theory of unsteady aerodynamics,[3–5] and also provide the basis for the recent developments.[6–16] However, this framework using potential flow is not complete and invokes a closure or auxiliary condition (e.g., the Kutta condition). Applying the Kutta condition at the sharp edges completes the framework by providing strengths of the newly shed vortices at these sharp edges. Consequently, one can use conservation of circulation to determine the value of the instantaneous bound circulation over the airfoil which dictates the generated lift force. Although this framework is indeed for a linearized, infinitely high Reynolds number flow at small angles of attack, it has been extensively used at low Reynolds numbers (e.g., biological flyers) relying on the facts that (i) there is no sharp stall (a smooth lift variation over a broad range of angles of attack[17,18]), (ii) the shear force contribution to the aerodynamic loads is unexpectedly minimal, as observed in the experimental study of Dikinson et al.[17] and the computational results of Wang[19] and Ramamurti and Sandberg.[20] Moreover, it has been believed for decades that, by allowing for sheets of vorticity bound the airfoil and in its wake, the classical thin airfoil theory does not completely ignore viscous effects; that is, the boundary layer over the airfoil and the viscous shear layer in the wake are represented by the infinitely thin bound and wake sheets of vorticity, respectively (see a detailed discussion by Sears[21]). However, the application of the Kutta condition to unsteady flows has been controversial (see Crighton[22] and the references therein).

*Assistant Professor, Henry Samueli Career Development Chair, Mechanical and Aerospace Engineering, AIAA Member.
†PhD Student, Mechanical and Aerospace Engineering, AIAA Student Member.

The need for an auxiliary condition alternative to Kutta's goes as early as the work of Howarth[23] with a research flurry on the applicability of Kutta condition to unsteady flows in the 1970's and 1980's.[22,24–27] This research was mainly motivated by the failure to capture an accurate flutter boundary.[28–30] Since structural dynamics could be captured with a good accuracy (e.g., exact beam theory), it has been deemed that the flaw stems from the classical unsteady aerodynamic theory, particularly the Kutta condition, as suggested by Chu[31] and Shen and Crimi[32] among others. Moreover, since these deviations occurred even at zero angle of attack (or lift),[33,34] it was inferred that there is a fundamental issue with such a theory that is not merely a higher-order nonlinear effect.[31] Therefore, there was almost a consensus that the Kutta condition has to be relaxed particularly at large frequencies, large angles of attack and/or low Reynolds numbers.[26,35,36] In fact, Orszag and Crow[37] regarded the full-Kutta-condition solution as "indefensible".

Interestingly, this dissatisfaction of the Kutta condition and the need for its relaxation is recently rejuvenated with the increased interests in the low Reynolds number, high frequency bio-inspired flight. Ansari et al.[9,38] asked for a modified version of the Kutta condition, particularly during rapid pitching near stroke reversals, to avoid creating artificially strong vortices; the envision was the pitch maneuver is so acute that the fluid may actually flow around the edge not along it. More recently, Pitt Ford and Babinsky[39] experimentally studied the leading edge vortex (LEV) dynamics over an impulsively started flat plate. They also developed a potential flow model that consists of a bound circulation, free LEVs and free trailing edge vortices. They determined the positions and strengths of the vortices by applying the γ_2-method[40] to their PIV measurements. Based on these values, they determined the value of the bound circulation that minimizes the deviation between the potential flow field and PIV measurements. Interestingly, during early stages, the optimum bound circulation was found to be the Kelvin's value (that satisfies Kelvin's law of conservation of circulation), which is considerably different from the Kutta's value (that satisfies the Kutta condition at the trailing edge). However, during later stages, the Kutta's value is closer to the optimum bound circulation than Kelvin's. In a similar setting, Hemati et al.[41] improved their previous varying-strength discrete vortex model[12] by relaxing the Kutta condition via applying optimal control theory to determine the strengths of the newly shed vortices that minimize the discrepancy between the potential-flow predicted forces and measurements; which was also found to be considerably different from Kutta's values.

Since the vorticity generation and lift development are essentially viscous processes, a purely inviscid theory of unsteady aerodynamics might be fundamentally flawed. In this effort, we revisit the unsteady boundary layer triple deck theory developed by Brown and Daniels[42] and Brown and Cheng[43] to develop a viscous extension (Reynold's number dependent) of Theodorsen's lift frequency response. We extend their effort (on a flat plate pitching around its mid-chord point) to the more general case of an arbitrarily-deforming thin airfoil (or time-varying camber), while correcting for a couple of their minor mistakes. Moreover, we perform a computational simulation using ANSYS Fluent for a harmonically pitching airfoil (NACA 0012) to assess the vaidity of the obtained results from the unsteady triple deck theory.

II. Triple Deck Theory

A. Steady Triple Deck

The triple deck theory has been originally devised to model local interactions near the trailing edge of an airfoil in steady flow due to the transition from a Blasius boundary layer, whose thickness is of order $Re^{-1/2}$, to a Goldstein near-wake, whose thickness is scaled as $Re^{-1/2}x^{1/3}$ where x is the distance downstream of the edge.[22] The triple deck structure has been proposed as a transition region between the two layers, which takes place over a short length of order $Re^{-3/8}$ (similar to Lighthill's supersonic shock-wave-boundary-layer interaction[44]), as shown in Fig. 1. Physically, upstream of the trailing edge, the flow decelerates inside a Blasius boundary layer due to its concomitant adverse pressure gradient (i.e., displacement thickness and pressure increase towards the edge). However, downstream of the edge, the wall is removed, hence, the fluid accelerates leading to a decrease in pressure. As such, a favorable pressure gradient develops in the transition region near the edge (i.e., in the triple deck). In other words, the triple deck structure represents a solution to the discontinuity of the viscous boundary condition at the edge;[42] from a zero tangential velocity on the airfoil to a zero pressure discontinuity on the wake center line.

Aerodynamicists modeled this transition through three decks (triple deck theory): (i) the upper deck which constitutes of an irrotational flow outside of the main boundary layer, (ii) the main deck which constitutes the main boundary layer (Blasius), and (iii) the lower deck, which is a sub-layer inside the main boundary layer, as shown in Fig. 1. As Crighton described in his seminal review article,[22] shortening of the

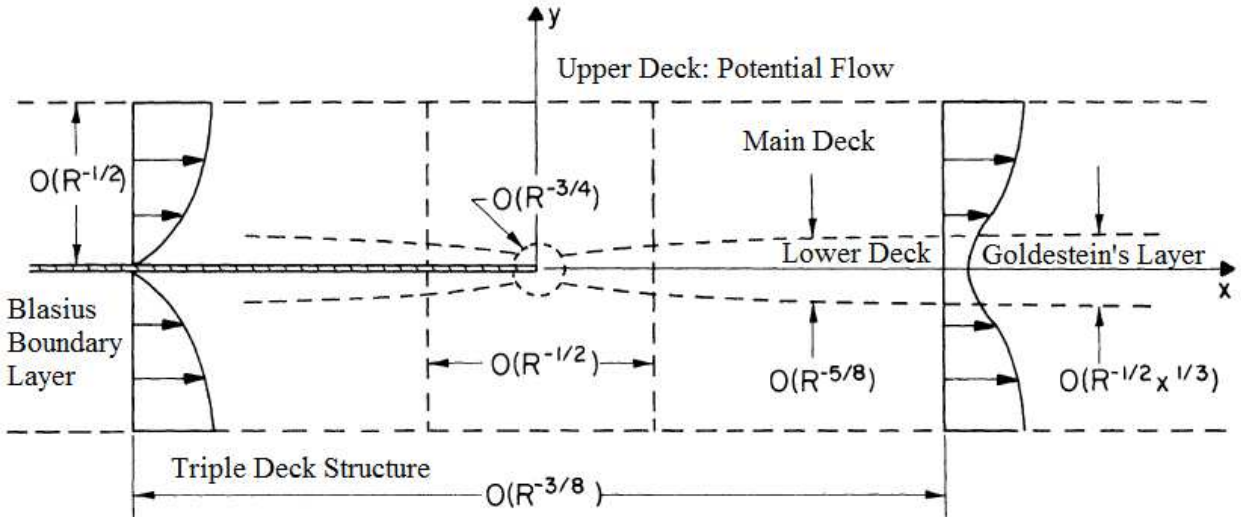

Figure 1: Triple deck structure and various flow regimes. Adapted from Messiter.[45]

x-scale makes the main deck ($Re^{-1/2}$) become inviscid, though rotational, and the viscous boundary layer equations apply only in the lower deck of thickness $Re^{-5/8}$. Also, Crighton noted that, unlike the thicker upstream boundary layer, the pressure inside the lower deck is unknown, but coupled with the irrotational pressure distribution in the upper deck. Note that the changes in the pressure and flow direction in the upper deck (potential flow) is determined by the thin airfoil theory, which are functions of x only. These changes are transmitted to the lower deck through the main deck (via Prandtl's boundary layer assumption $\frac{\partial p}{\partial y} = 0$). Therefore, the Prandtl boundary layer equations are applied in the lower deck, driven by the pressure of the upper deck. That is, instead of having an inhomogeneous boundary layer equations driven by an external pressure, the lower deck boundary layer equations are homogeneous, but coupled with x-perturbations in the upper deck. The triple deck theory results in the the following correction of the Blasius skin friction drag coefficient

$$C_D \simeq \frac{1.328}{\sqrt{Re}} + \frac{2.66}{Re^{7/8}}$$

which is in an astonishingly good agreement with both Navier-Stokes simulations and experiments down to $Re = 10$ and even lower.

Stewartson[46] and Messiter[45] were the first to develop the triple deck theory for a flat plate in a steady flow at zero angle of attack. Brown and Stewartson[47] extended such a work for a non-zero angle of attack in the order of $Re^{-1/16}$. This is the range of interest because (i) if α is much lower, then the flow can be considered as a perturbation to the case of $\alpha = 0$ and (ii) if it is much higher, then the flow would separate well before the trailing edge. Over this range, the resulting adverse pressure gradient is of the same order as the favorable pressure gradient in the triple deck, leading to separation in the immediate vicinity of the trailing edge, which is called *Trailing Edge stall*. Brown and Stewartson[47] formulated such a problem and showed that the flow enters the triple deck on both sides separately and the flow in the lower deck is governed by partial differential equations that are solved numerically for each value of $\alpha_e = Re^{1/16}\lambda^{-9/8}\alpha$, where $\lambda = 0.332$ is the Blasius skin-friction coefficient. Jobe and Burggraf[48] and Veldmann and Van de Vooren[49] solved the $\alpha_e = 0$ case, while Chow and Melnik[50] solved the case $0 < \alpha_e < 0.45$ and concluded that the flow will separate from the suction side of the airfoil from the trailing edge at $\alpha_e = 0.47$ (trailing edge stall angle). We remark that this α_e value for trailing edge stall corresponds to quite a small value for the actual angle of attack; $\alpha = 3.1° - 4.2°$ for $Re = 10^4 - 10^6$.

B. High-Frequency Unsteady Triple Deck

While the steady triple deck theory has been well exposed to engineers and fluid dynamicists (being taught at regular graduate courses in fluid mechanics), its unsteady extension does not enjoy the same fame. Brown and Daniels[42] were the first to extend the steady triple deck theory to the case of a high-frequency, small-amplitude oscillatory pitching flat plate. Unlike the steady case, there is a Stokes layer near the wall that

is of order $\sqrt{\nu/\omega}$ where the viscous term is balanced by the time-derivative term in the equations. Brown and Daniels assumed that the Stokes layer and the lower deck have the same thickness, which results in $k_c = O(Re^{1/4}) = \frac{1}{\epsilon^2}$, where they used $k_c = 2k$ as a non-dimensional frequency; the reduced frequency based on the chord length. They argued that this range is the right range of interest because (i) if k_c is much smaller, then the flow can be considered as a perturbation to the steady case with a non-zero α (i.e., to the work of Brown and Stewartson[47]) and (ii) if it is much larger, then the flow variations may be too rapid to preserve the triple deck structure. In fact, this results in k values that are too large for engineering applications; $k \simeq 5 - 15$ for $Re = 10^4 - 10^6$. Then, the matching between the adverse pressure gradient due to oscillation and the triple deck favorable pressure gradient results in a pitching amplitude $O(Re^{-9/16})$, which is also ridiculously small for engineering applications; $\simeq 0.02^\circ - 0.32^\circ$ for $Re = 10^4 - 10^6$. Indeed, their work is for very high-frequency, very small-amplitude oscillations.

Brown and Daniels[42] determined a Reynolds-number-dependence for the arbitrary constant in the outer flow, which dictates the circulation around the aerofoil. Its limit as $Re \to \infty$ is determined by the Kutta condition (zero loading) at the trailing edge. However, the matching between the triple deck and the outer flow provides a correction for this Kutta's circulation, which is $O(Re^{-3/8})$. In their formulation, Brown and Daniels[42] setup the triple deck structure near the trailing edge and a perturbed Blasius boundary layer with an inner Stokes layer upstream of the trailing edge, as shown in Fig. 2. However, unlike the steady case, the solution of the perturbed Blasius boundary layer could not be matched with the main deck of the triple deck structure. Therefore, Brown and Daniels introduced a transition region, whose length is $O(Re^{-1/4})$, between the perturbed Blasius boundary layer and the triple deck; called the *fore deck*. It has similar structure to that upstream of the triple deck; outer potential flow, main boundary layer, and an inner Stokes layer, as shown in Fig. 2. Also, it is noteworthy to remark that the velocity profile of the perturbed Blasius boundary layer does not have to satisfy the no-slip boundary condition because such a condition is left to the inner Stokes layer.

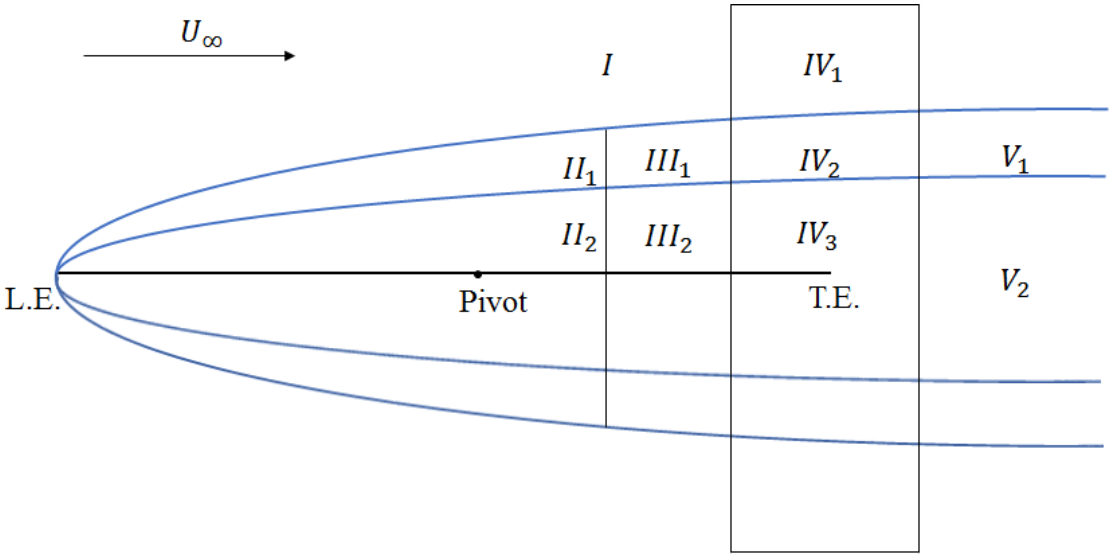

Figure 2: High frequency triple deck (adopted from the work of Brown and Daniels 2). I: potential flow, II: modified Blasius and inner Stokes layer, III: the fore deck, IV: the triple deck, and V: modified Goldstein wake.

It is interesting to remark that, up to first-order, the time-derivative term does not appear in the main deck equations, but still shows up in the lower deck ones. Brown and Daniels[42] could not solve the partial differential equations governing the flow in the lower deck, but managed to determine the following linearized solution for a flat plate pitching around its mid-chord point ($\alpha(t) = A_\alpha \cos \omega t$) [a]

$$C_L(t) = \underbrace{-\frac{3}{2}\pi A_\alpha k \sin \omega t}_{\text{Potential Flow}} + \underbrace{\frac{1}{2}\pi A_\alpha \frac{k^{3/2}}{\sqrt{\lambda} Re^{1/4}} \cos(\omega t - \pi/4)}_{\text{Viscous Correction}} \tag{1}$$

[a]Note that the first term in Eq. (1) representing potential-flow solution is considered in the limit to high-frequencies (i.e., The Theodorsen function $C(k) \to \frac{1}{2}$ and the α-terms are neglected with respect to the $\dot{\alpha}$-terms).

That is, the viscous correction reaches up to 10% for $k = 1$ and $Re = 1,000$. Also, it lags behind the inviscid leading term by $\pi/4$ phase.

III. Proposed Model: Low-to-Moderate-Frequency Unsteady Triple Deck

In this subsection, we extend the work of Brown and Cheng[43] to an arbitrarily deforming thin airfoil and correct for few minor mistakes in their derivation, however, we mainly follow their perturbation analysis. More importantly, we use the obtained results, within a describing function formulation[51] assuming weakly-nonlinear dynamics, to provide a viscous extension of the classical Theodorsen's lift frequency response. Following Brown and Cheng,[43] we concern our efforts with oscillation frequencies in the range $0 < k_c << Re^{1/4}$, which is quite relevant to engineering applications. Luckily, over this range of relatively-small frequencies, not only the main deck equations are void of the time-derivative term, up to first-order, but also the lower deck ones; that is, the lower deck equations are quite similar to those of the steady case at a non-zero α (studied by Brown and Stewartson[47]) with a proper definition for the equivalent steady angle of attack. However, we emphasize that this approach is not a quasi-steady solution; although the time-derivative does not show up in the lower deck equations, the correspondence with the steady equations implies an equivalent angle of attack that is dependent on the oscillation frequency, as will be shown below. Therefore, the lower deck system is dynamical (i.e., posses a non-trivial frequency response). In fact, even with no time-derivative term in the lower deck equations, it is not obvious how the steady results of Brown and Stewartson[47] can be readily applied because the upstream flow is unsteady with Stokes layers in both the perturbed Blasius layer and the fore deck; as there seems to be a mismatch between the fore deck unsteady flow and the triple deck "quasi-steady" flow. However, following Brown and Cheng,[43] this issue is circumvented by inserting a second fore deck between the first fore deck and the triple deck, as shown in Fig. 3. As such, the numerical results of Chow and Melnik[50] to the steady problem of Brown and Stewartson[47] could be readily used with an equivalent steady angle of attack. Since the equivalent steady angle of attack α_e is proportional to $A_\alpha k^2$, and the steady triple deck formulation of Brown and Stewartson[47] is valid for $\alpha = O(Re^{-1/16})$, our unsteady formulation (similar to Brown and Cheng's[43]) is valid for $A_\alpha k^2 = O(Re^{-1/16})$, which is quite relevant to engineering applications (e.g., $Re \simeq 10,000$, $k \simeq 0.5$, and $A_\alpha \simeq 16°$).

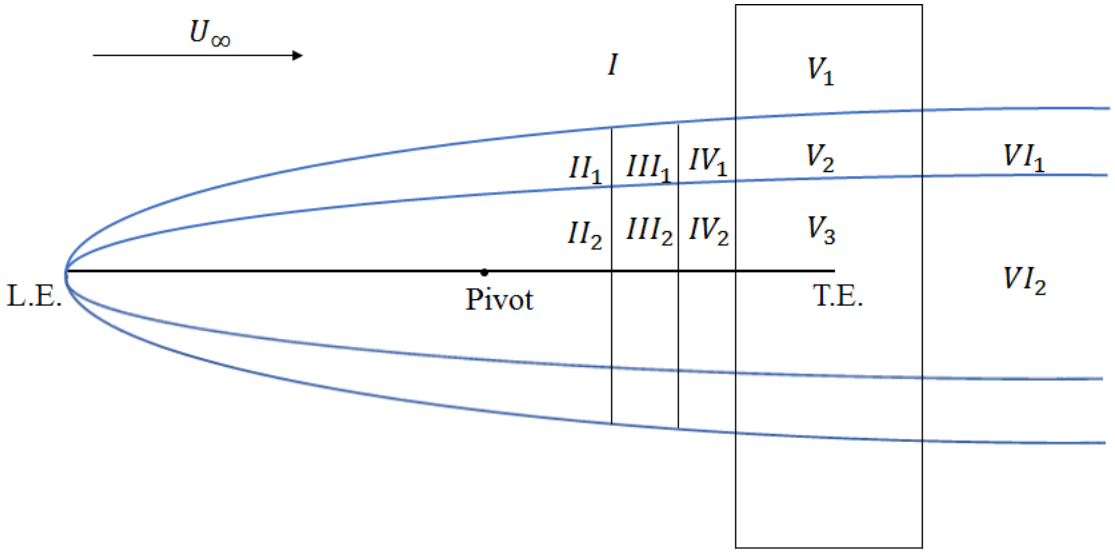

Figure 3: Low frequency triple deck. I: potential flow, II: modified Blasius and inner Stokes layer, III: the first fore deck, IV: the second fore deck, V: the triple deck, and VI: modified Goldstein wake.

A. Approach

Consider an arbitrarily deforming thin airfoil (i.e., of time-varying camber) in the presence of a uniform stream U, as shown in Fig. 4. In classical thin airfoil theory,[52–54] it is typical to assume the following series solution for the pressure distribution over the upper surface, which automatically satisfies the Kutta

condition (zero loading at the trailing edge)

$$P(\theta,t)=\rho\left[\frac{1}{2}a_0(t)\tan\frac{\theta}{2}+\sum_{n=1}^{\infty}a_n(t)\sin n\theta\right] \tag{2}$$

where ρ is the fluid density, θ is related to x via $x=b\cos\theta$, b is the semi-chord length, and a_0 represents

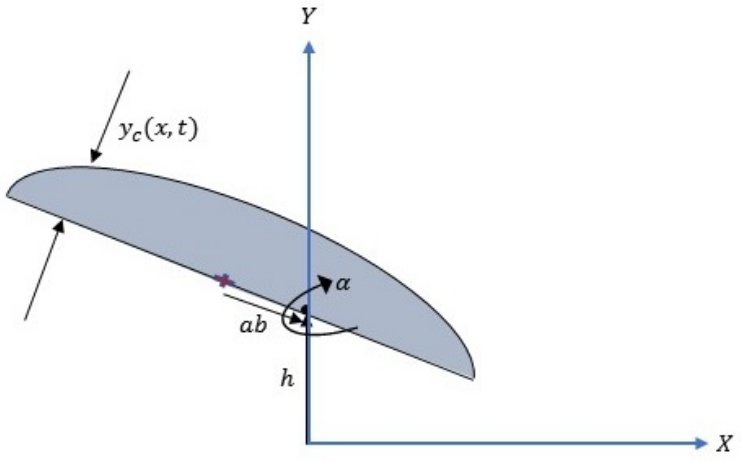

Figure 4: Flexible thin airfoil

the leading-edge singularity. The pressure on the lower side is given by the negative of Eq. (2). Moreover, if the plate's normal velocity v_p is written as

$$v_p(\theta,t)=\frac{1}{2}b_0(t)+\sum_{n=1}^{\infty}b_n(t)\cos n\theta$$

then, the no-penetration boundary condition will provide a means to determine all the coefficients a_n's (except a_0) in terms of the plate motion kinematics (b_n's) as shown by Robinson and Laurmann,[54] pp. 491

$$a_n(t)=\frac{b}{2n}\dot{b}_{n-1}(t)+Ub_n(t)-\frac{b}{2n}\dot{b}_{n+1}(t),\quad\forall\, n\geq 1 \tag{3}$$

The determination of a_0 is more involved in the sense that it requires solving an integral equation, which cannot be solved for arbitrarily time-varying wing motion. It has been solved for some common inputs; e.g., step change in the angle of attack resulting in the Wagner's response,[3] simple harmonic motion resulting in Theodorsen's frequency response,[4] and sharp-edged gust.[55] Since the focus of this work is to provide a viscous extension to Theodorsen's frequency response, consider the simple harmonic motion

$$v_p(\theta,t)=V_p(\theta)e^{i\omega t};\quad V_p(\theta)=\frac{1}{2}B_0+\sum_{n=1}^{\infty}B_n\cos n\theta$$

where the spatially-varying amplitude $V_p(\theta)$ may be complex and ω is the oscillation frequency. Then, a_0 is written as,[54] pp. 496 [a]

$$a_0(t)=U(B_0+B_1)C(k)e^{i\omega t}-Ub_1(t) \tag{4}$$

where $C(k)$ is the Theodorsen's frequency response function, which depends on the reduced frequency $k=\frac{\omega b}{U}$. Finally, the potential-flow lift force and pitching moment (positive pitching up) at the mid-chord point are written as

$$L_P=-\pi\rho b(a_0+a_1)\ \text{ and }\ M_{0_P}=\frac{\pi}{2}\rho b^2(a_2-a_0) \tag{5}$$

[a]Note that the presentation of Robinson and Laurmann is adapted to a more common and modern notation.

Having introduced above the potential-flow setup of the problem, let us induce a trailing-edge singularity term in the pressure distribution shown in Eq. (2) as

$$P(\theta,t) = \rho\left[\frac{1}{2}a_0(t)\tan\frac{\theta}{2} + \sum_{n=1}^{\infty} a_n(t)\sin n\theta + \frac{1}{2}B_{\rm v}(t)\cot\frac{\theta}{2}\right] \tag{6}$$

It should be emphasized that the no-penetration boundary condition, alone, cannot determine $B_{\rm v}$ and an auxiliary condition is invoked to determine its value within the framework of potential flow. In particular, the Kutta condition dictates that $B_{\rm v} = 0$ resulting in the potential-flow solution introduced above. In this effort, similar to the work of Brown and Cheng,[43] we will use the unsteady triple deck theory, exploiting the vanishing of the time-derivative term from the boundary layer equations, to determine $B_{\rm v}$ in terms of k and Re. Then, the viscous correction (contribution of $B_{\rm v}$) to lift and pitching moment will be written as

$$L = -\pi\rho b(a_0 + a_1 + B_{\rm v}) \;\text{ and }\; M_0 = \frac{\pi}{2}\rho b^2(a_2 - a_0 + B_{\rm v}) \tag{7}$$

Approaching the trailing edge ($\theta \to 0$ or $\hat{x} = \frac{x}{b} \to 1$), the inviscid pressure (with the $B_{\rm v}$ term) is written as

$$P(\hat{x}\to 1;t) = \rho\left[\left(\frac{1}{2}a_0(t) + 2\sum_{n=1}^{\infty} n a_n(t)\right)\sqrt{\frac{1-\hat{x}}{2}} + \frac{B_{\rm v}(t)/2}{\sqrt{\frac{1-\hat{x}}{2}}}\right] \tag{8}$$

which reduces to that in Brown and Stewartson[47] as $k \to 0$ and to that in Brown and Daniels[42] as $k \to \infty$, with $a_n = 0$ for all $n > 2$ for their case of a pitching flat plate. Similar to both efforts, scaling is devised such that the inviscid pressure near the trailing edge, given in Eq. (8), is of the same order as that of the triple deck; i.e., $O(\epsilon^2)$ when $1 - \hat{x} = O(\epsilon^3)$. Assuming $\epsilon = Re^{-1/8} << 1$, this scaling argument implies $(0.5A_\alpha)k_c^2 = O(\sqrt{\epsilon}) = O(Re^{-1/16})$. Brown and Daniels[42] chose $k_c = O(\epsilon^{-2}) = O(Re^{1/4})$ so that the thickness of the Stokes layer $\delta_{\rm Stokes} = O(\sqrt{\nu/\omega}) = O(k_c^{-1/2}\epsilon^4)$ is of the same order as that of the inner deck $O(\epsilon^5)$. In contrast, Brown and Cheng[43] chose $k_c < O(\epsilon^{-2})$ so that the Stokes layer is thicker than the inner deck ($O(\epsilon^5)$), but thinner than the main deck ($O(\epsilon^4)$).

Recall the steady pressure distribution near the trailing edge, given in (2.2) of Brown and Stewartson,[47] and re-write it in the terminology of this paper, we have

$$P_s(\hat{x}\to 1) = \rho U^2\alpha_s\left[-\sqrt{\frac{1-\hat{x}}{2}} + \frac{B_s/2}{b\sqrt{\frac{1-\hat{x}}{2}}}\right]\text{sgn}(y) \tag{9}$$

where α_s and B_s are the equivalent steady angle of attack and $B_{\rm v}$. The unsteady inviscid pressure given in Eq. (8) has the same form as the steady one given in Eq. (9) with

$$\alpha_s(t) \equiv \frac{1}{U^2}\left|\frac{1}{2}a_0(t) + 2\sum_{n=1}^{\infty} n a_n(t)\right| \;\text{ and }\; B_{\rm v}(t) \equiv -\left(\frac{1}{2}a_0(t) + 2\sum_{n=1}^{\infty} n a_n(t)\right)\frac{B_s(t)}{b} \tag{10}$$

This comparison along with the fact that the time-derivative term does not enter the triple deck equations points to the possibility of directly using the steady solution by Chow and Melnik[50] of the inner deck equations for the unsteady case with the equivalence shown above; valid in the range $0 < k_c < O(Re^{1/4})$. In the above equivalence, if the term $\frac{1}{2}a_0(t) + 2\sum_{n=1}^{\infty} n a_n(t)$ is negative, then the top of the oscillating thin airfoil will correspond to the top of the steady plate and if is positive, then the top of the oscillating thin airfoil should correspond to the bottom of the steady plate. In either case, α_s would be positive. In fact, this correspondence has lead to the following interesting behavior. While there is always a significant lift decrease at the trailing edge stall angle in the steady case, there can be either increase or decrease in the unsteady lift when α_s reaches the trailing edge stall value, as shown by Brown and Cheng.[43]

Note that the numerical solution by Chow and Melnik[50] provides B_e as a nonlinear function of α_e, which is represented here in Fig. 5, where

$$\alpha_e = \alpha_s\epsilon^{-1/2}\lambda^{-9/8} \;\text{ and }\; B_s = 2b\epsilon^3\lambda^{-5/4}B_e(\alpha_e) \tag{11}$$

In other words, they provide $B_s = B_s(\alpha_s)$. Thus, the instantaneous values of $a_n(t)$, determined from the airfoil kinematics via the no-penetration boundary condition given in Eq. (3,4), will define the equivalent

steady angle of attack α_s according to (10), which will lead to $B_s(\alpha_s(t))$ via the results of Chow and Melnik.[50] Finally, B_v will be determined from B_s and the a_n's according to (10), which represents the viscous correction to the Kutta condition and consequently to the lift and moment. It should be noted that this procedure admits arbitrary time variation of the airfoil camber (not necessarily harmonic); only a_0 should be modified accordingly instead of using (4). Nevertheless, because there might not be exact closed-form expressions for $a_0(t)$ due to other kinematics (e.g., step input), we recommend using (4) to construct a viscous frequency response (describing function[51]), assuming weakly nonlinear response, and then using the Fourier transform to obtain the viscous lift force and pitching moment due to an arbitrarily time-varying camber, as shown by Garrick[56] and Bisplinghoff et al.,[53] pp. 282-283.

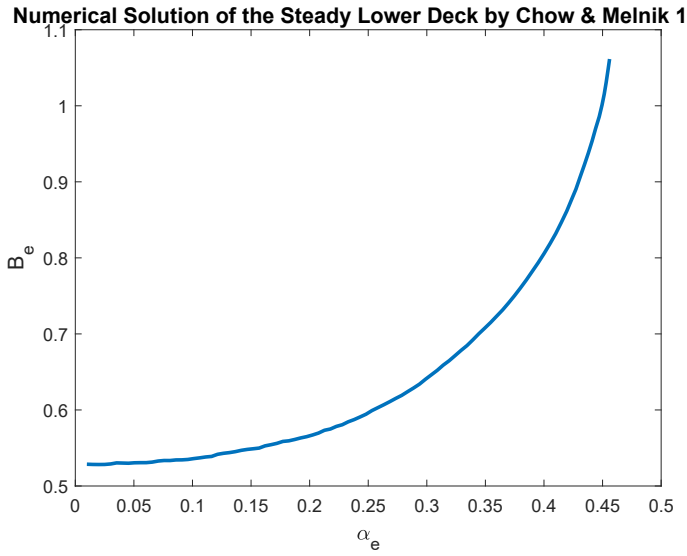

Figure 5: Numerical solution of the steady lower deck equations for $0 < \alpha_e < 0.45$, adapted from Chow and Melnik.[50]

B. Viscous Frequency Response (Describing Function)

The above approach can be used to construct a viscous extension of Theodorsen's function at a given Reynolds number. For practical use, we opt to show such an extension for a pitching plunging flat plate. In this case, the normal velocity of the plate (assuming small disturbances $\dot{h}$ and α) is written as

$$v_p(x,t) = \dot{h}(t) - \dot{\alpha}(t)(x - ab) - U\alpha, \quad -b \le x \le b \tag{12}$$

where h is the plunging displacement (positive upward) and α is the pitching angle (angle of attack, positive clockwise), and ab represents the chordwise distance from the mid point to the hinge point, as shown in Fig. 4. This type of kinematics results in

$$b_0(t) = 2\left[\dot{h}(t) + ab\dot{\alpha}(t) - U\alpha\right] = 2v_{1/2}(t), \quad b_1(t) = -b\dot{\alpha}(t) \text{ and } b_n = 0 \; \forall n > 1$$

where $v_{1/2}$ is the normal velocity of the mid-chord point. As such, for the harmonic motion

$$h(t) = Hbe^{i\omega t} \text{ and } \alpha(t) = A_\alpha e^{i\omega t} \tag{13}$$

Eqs. (3,4) result in the following coefficients

$$a_0(t) = U\left[2V_{3/4}C(k)e^{i\omega t} + b\dot{\alpha}(t)\right], \quad a_1(t) = b\dot{v}_{1/2} - bU\dot{\alpha}(t), \quad \text{and} \quad a_2(t) = -\frac{b^2\ddot{\alpha}(t)}{4} \tag{14}$$

where $v_{3/4}(t) = V_{3/4}e^{i\omega t}$ is the normal velocity at the three-quarter-chord point. In the common classification proposed by Theodorsen,[4] the coefficient a_0 represents the circulatory contribution while the other two

coefficients a_1, a_2 represent the non-circulatory contribution. The lift coefficient is then written as

$$C_L(t) = -\frac{\pi}{U^2}\left[a_0(t) + a_1(t) + B_{\rm v}(t)\right] = \underbrace{\underbrace{-\pi\frac{b\dot{v}_{1/2}(t)}{U^2}}_{\text{Non-circulatory}} + \underbrace{2\pi\alpha_{3/4}(t)C(k)}_{\text{Circulatory}}}_{\text{Potential Flow Solution}} - \underbrace{\pi\hat{B}_{\rm v}(t)}_{\text{Viscous Correction}} \tag{15}$$

where $\hat{B}_{\rm v} = \frac{B_{\rm v}}{U^2}$, $\alpha_{3/4}$ is the local angle of attack at the three-quarter-chord point, as recommended by Pistolesi theorem,[52] pp. 80, and the multiplication $\alpha_{3/4}(t)C(k)$ is interpreted after writing $\alpha_{3/4}(t) = \overline{\alpha_{3/4}}e^{i\omega t}$, where $\overline{\alpha_{3/4}}$ may be complex number, as

$$\alpha_{3/4}(t)C(k) = \Re\left(\overline{\alpha_{3/4}}C(k)e^{i\omega t}\right)$$

where $\Re(.)$ denotes the real part of its complex argument.

Recall that if $u(t) = Ae^{i\omega t}$ is the input to a linear dynamical system whose frequency response is $G(i\omega)$, then the output is simply written as $y(t) = A|G(j\omega)|e^{i\omega t + \angle G(j\omega)}$.[57] The describing function technique represents an extension to the frequency response concept for weakly nonlinear systems.[51] In this technique, only the response at the fundamental frequency is considered and the higher harmonics are neglected. As such, the response of a weakly nonlinear system to the input $u(t) = Ae^{i\omega t}$ is approximated as $y(t) = Y(A,\omega)e^{i\omega t + \phi(A,\omega)}$. That is, unlike linear systems, the magnitude and phase of the transfer function depend on the input amplitude. Using such a technique we provide below a viscous extension to Theodorsen's frequency response; i.e., the frequency response between the quasi-steady lift (input) and the viscous circulatory lift (output). Figure 6 shows a block diagram for the dynamics of the unsteady viscous circulatory lift. Indeed, the system is weakly nonlinear; only one nonlinear element whose contribution is minimal with respect to the main linear contribution.

Let k and Re be given. Then, the quasi-steady lift coefficient (input to our sought flow dynamical system) is written as

$$C_{L_{QS}}(t) = 2\pi\alpha_{3/4}(t)$$

Also, the coefficients a_0, a_1, and a_2 are given from Eq. (14). Thus, α_s can be obtained accordingly from Eq. (10). Care should be taken when applying Eq. (10). It should be applied instantaneously; at each time instant, the right hand side containing the a's coefficients is complex. The instantaneous $\alpha_s(t)$ should be given by

$$\alpha_s(t) = \frac{1}{U^2}\left|\Re\left[\frac{1}{2}a_0(t) + 2a_1(t) + 4a_2(t)\right]\right|$$

As such, the equivalent angle of attack $\alpha_e(t)$ for the numerical solution of Chow and Melnik[50] is obtained from Eq. (11) with $\epsilon = Re^{-1/8}$. Note that if $\alpha_e(t)$ exceeds 0.47, then the simulation should be terminated because such a value implies trailing edge stall beyond which the current analysis is not valid. Using, Fig. 5, one can obtain $B_e(t)$, which in turn is substituted in Eq. (10) to determine the viscous correction $B_{\rm v}(t)$. Finally, the unsteady viscous circulatory lift coefficient is determined from Eq. (15) by excluding the first term, i.e.,

$$C_{L_C}(t) = \Re\left[2\pi\alpha_{3/4}(t)C(k) - \pi\hat{B}_{\rm v}(t)\right] \tag{16}$$

and a spectral analysis (e.g., FFT) is applied to $C_{L_C}(t)$ to extract its relative amplitude and phase shift with respect to $C_{L_{QS}}(t)$.

Following the above procedure, we construct frequency responses of the unsteady, viscous, circulatory lift coefficient C_{L_C} at different Reynolds numbers, which are shown in Fig. 7 in comparison to Theodorsen's. Intuitively, as Re increases, the viscous response approaches the inviscid Theodorsen's response and vice versa. In particular, viscosity leads to a significantly more phase lag, which is an important characteristic to capture; note that the flutter instability, similar to any typical limit cycle oscillation, is mainly dictated by when energy is added/subtracted during the cycle. That is, the phase difference between the applied loads (aerodynamic loads) and the system motion (e.g., angle of attack) plays a crucial role in dictating the stability boundary. We recall the experimental results of Bass et al.[27] who conducted a water tunnel experiment for a NACA 16-012 undergoing pitching oscillations around its quarter-chord point in the range of $0.5 < k < 10$ and $Re = 6,500 - 26,500$. They compared their force measurements to Theodorsen's potential flow frequency response. They found bad agreement in the range $0.5 < k < 2$ where the most pronounced

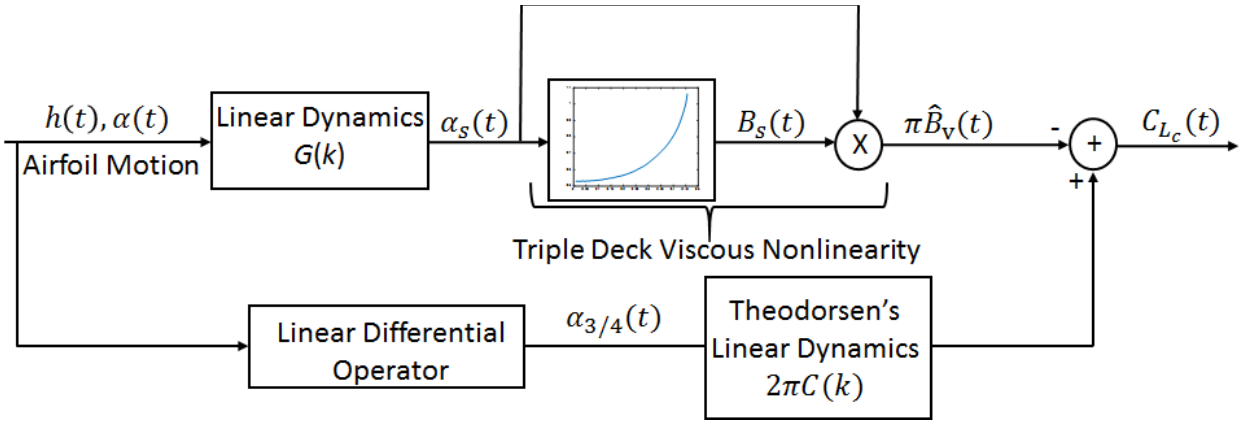

Figure 6: A block diagram showing the different components constituting the dynamics of the viscous circulatory lift.

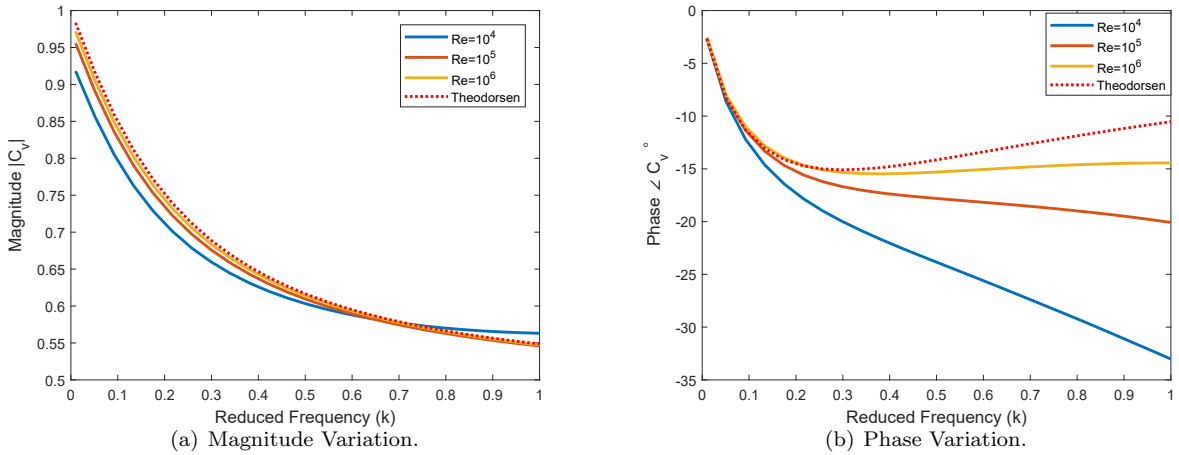

(a) Magnitude Variation. (b) Phase Variation.

Figure 7: Comparison between the frequency responses of the unsteady, viscous, circulatory lift coefficient C_{L_C} at different Reynolds numbers and that of the potential-flow circulatory lift coefficient (i.e., Theodorsen's).

boundary layer activity is observed and the flow near trailing edge being separated and alternating around the trailing edge. They concluded that adding a phase lag of -30° to the Theodorsen's $C(k)$ will make it match the experimental results over this range, which supports the results shown in Fig. 7. Based on this discussion, we suggest using the obtained viscous frequency responses in place of Theodorsen's for a more accurate, yet efficient, estimate of the flutter boundary.

IV. Computational Simulation

A. Numerical Method

In order to study the effect of viscosity on the transfer function, the 2D incompressible URANS equations have been numerically solved using finite volume based software package ANSYS FLUENT. To this end, the well-known turbulence model, $KWSST$ was used. This model showed promising results in solving external flows at high Reynolds number, particularly in airplane aerodynamic applications. The detailed formulation of this model can be found in the efforts of its developers.[58,59] As the Reynolds number is high and the amplitude of the deflection is small in this investigation and no severe pressure gradient and separation is expected, $KWSST$ would be quite suitable.

In relation to the numerical setup, the pressure velocity coupling is dealt with by the SIMPLE algorithm, and since the flow is incompressible, the pressure-based solver is utilized. The properties of the flow at inlet was used to calculate the dimensionless quantities. All the spatial discretization are second order upwind. Implicit second order discretization is chosen for transient terms. The convergence criterion for all the variables are set to be 10^{-6} at each time step. To select an appropriate value for the time step, three numerical simulations are performed. In each case, the time step is set to be $500/period$, $250/period$ and $150/period$ respectively. It is found that 250 sample per each cycle is sufficient to obtain well-converged results. In each simulation, the number of cycles are chosen to be sufficient for a periodic lift pattern to establish.

B. Computational Domain

The O-Type farfield located $25c$ away from the solid body has been implemented for grid generation around the standard NACA 0012 airfoil with sharp trailing edge. In return of closing the blunt trailing edge of the original NACA 0012, the thickness of the airfoil altered to 11.9%.

To construct the dynamic mesh due to the airfoil motion, the computational domain is divided into three rings as shown in Fig. 8. The inner ring (red), which encloses the airfoil, has the radius of $6c$. In this region hybrid mesh is used such that a boundary layer structure dense mesh near the airfoil guarantees $y+ < 1$, in conjunction with the unstructured tri mesh attached to it to fill this region. The distance of the first layer of the mesh was set to be $10^{-5}c$ with 1.1 growth factor, and the total of 300 mesh points were used on each side of the airfoil. A size function has been used to ensure that the unstructured mesh in the inner ring is dense enough to capture the shed vortices if needed. Both the structure boundary layer grids and unstructured grids close to the trailing edge and leading edge are shown in Fig. 9. The whole inner ring including the airfoil undergo the pitching movement analogous to a rigid body inside its outer domain. No dynamic mesh is allowed in this region to ensure that the grids near the airfoil maintain their fine configuration and quality as they were before the movement.

On the other side, the outer ring located at $25c$ away from the airfoil is stationary as if no movement is happening inside the domain. These fixed meshes in the vicinity of the farfield edges certify that the boundary conditions in the farfiled are imposed correctly in the solution procedure. The intermediate ring plays the main role for the dynamic mesh approach. The inner radius of this ring is $6c$ and the outer radius is $18c$; thus it occupies a large region inside the main domain. Both remeshing and deforming techniques are utilized to damp the deformations in the region caused by the movement of the inner ring and absence of movement in the outer ring. A User Defined Function is attached to the solver to impose the arbitrary movement to the airfoil (pitching) and prevent high skewness in the dynamic mesh Zone. The advantage of this method may not be sensible when deflections are small, yet it demonstrates its ability in damping the mesh movements when the amplitude of deflection is significant. The large size of the intermediate region gives enough room to it for handling the deflections. It has to be pointed out that the position of each ring has been chosen based on numerous simulations were done. The total number of grids is roughly 2×10^5.

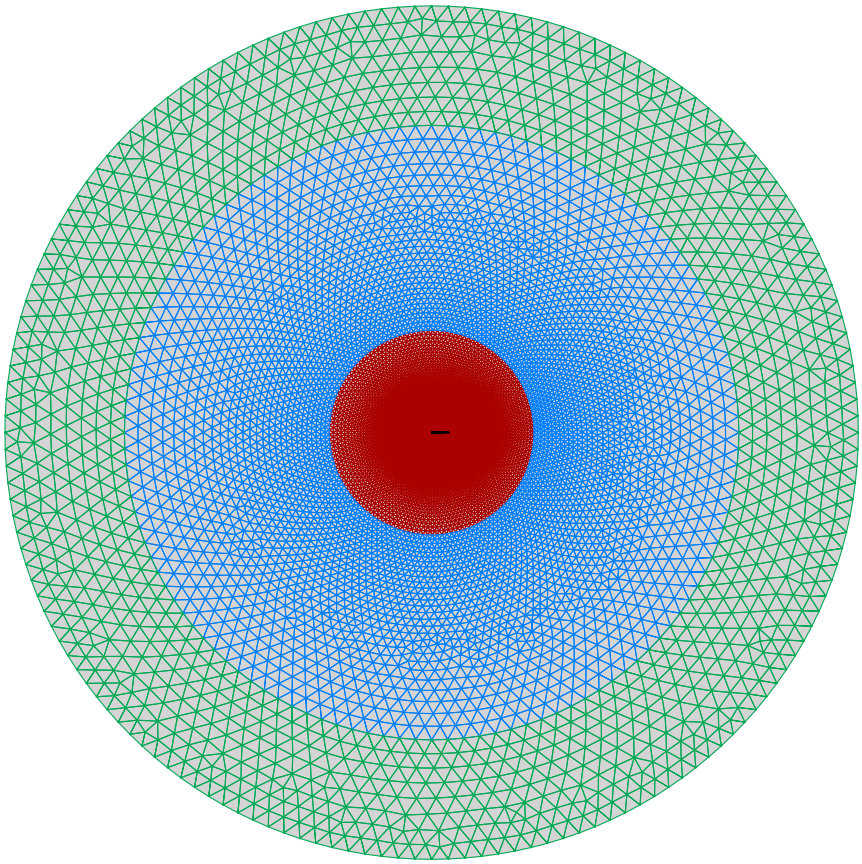

Figure 8: O-Type mesh around the airfoil

Mesh independence study has been done by running another case in which the grids were twice denser and no alternation in the results has been observed. Thus, the aforementioned mesh configuration was utilized in the simulations.

C. Boundary Conditions

Since the flow was assumed to be incompressible, the boundary conditions at farfield were velocity inlet and pressure outlet corresponding to left semi-circle and right semi-circle respectively. The chord length of the airfoil was $18cm$ and the magnitude of the velocity at the inlet boundary was $50m/s$ and $25m/s$ for two different Reynolds number. In order to set the Reynolds number to $100,000$ and $1,000,000$, the fluid properties were manipulated. The turbulent intensity of the flow was 0.1% and the guage pressure at outlet boundary condition set to zero. No slip boundary condition is used for airfoil prescribed to a harmonic sinusoidal motion

$$\alpha = A_\alpha \sin \omega t \quad , \quad \dot{\alpha} = A_\alpha \omega \cos \omega t$$

with a pitching amplitude of 3 degrees to ensure that the airfoil is in pre-stall regime.

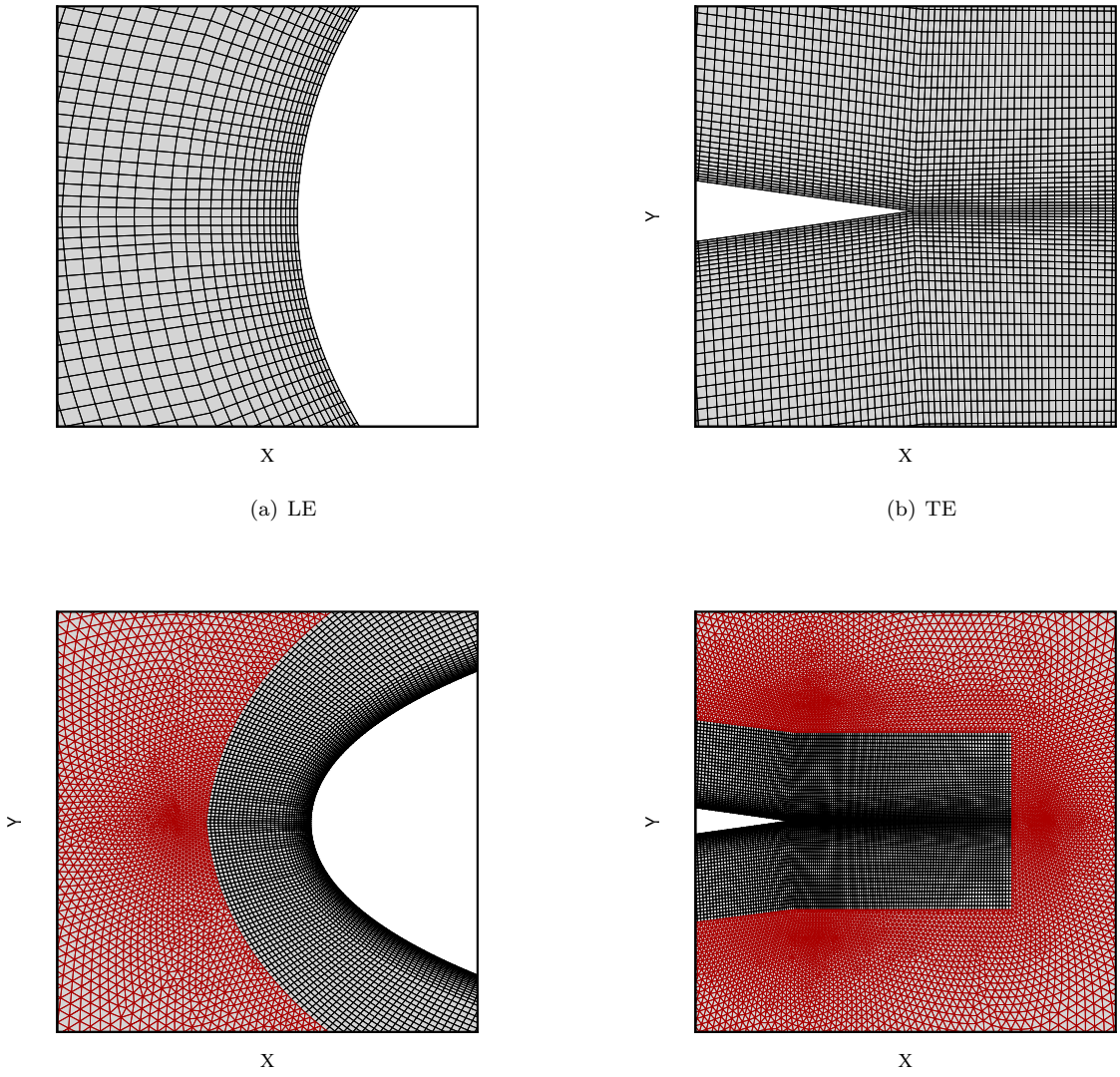

(a) LE (b) TE

(c) LE Hybrid mesh (d) TE Hybrid mesh

Figure 9: Mesh topology near the leading edge and trailing edge of the airfoil

D. Method of Finding the Transfer Function

In this study, the transfer function was assessed based on the Theodorsen approach as it was reflected in the potential flow solution part of the Eq. 15. Consider the coordinate system in Fig. 10 which the α is in +x direction, $\dot{\alpha}$ is in $+y$ direction, and $\ddot{\alpha}$ is in $-x$ direction. By decomposing all the terms in each lift coefficient, and adding or subtracting them as vectors, the gain and the phase of the transfer function is obtained. Note that for both the input (α) and the output ($C_{L_{\text{tot}}}$), phase and amplitude is needed which are calculated by taking Fast Fourier Transform of the $\alpha - time$ and $C_{L_{\text{tot}}} - time$ data from the simulation results. It is evident that for attaining better accuracy in the results of Fourier transform, both tiny time step and sufficient number of cycles are essential.

E. Results

Figure 11 shows the results from our computational setup presented above for the frequency response between the quasi-steady lift coefficient as an input and the unsteady circulatory lift as an output, at two different Reynolds numbers. The figure also shows Theodorsen's for comparison. The obtained trends corroborate

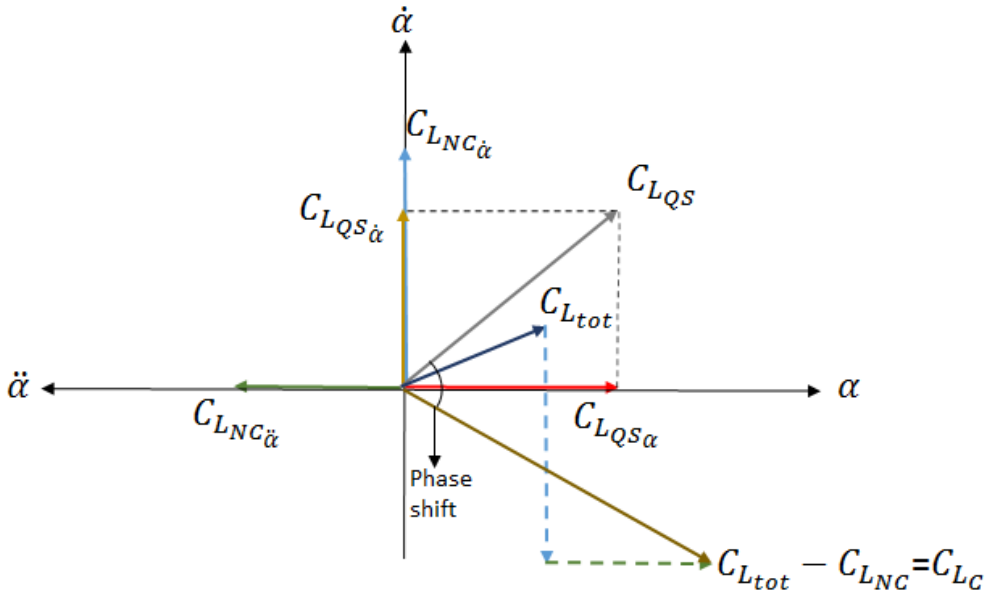

Figure 10: The coordinate system that describes the method of finding the phase and amplitude of the transfer function.

the theoretical findings discussed above. That is, at lower Reynolds numbers and higher frequencies, there is a significant deviation from Theodorsen's phase prediction. The computational results exaggerate these deviations even more. These deviations may significantly affects the prediction of an instability boundary. Therefore, it may be the reason behind our retarding capability in predicting flutter.

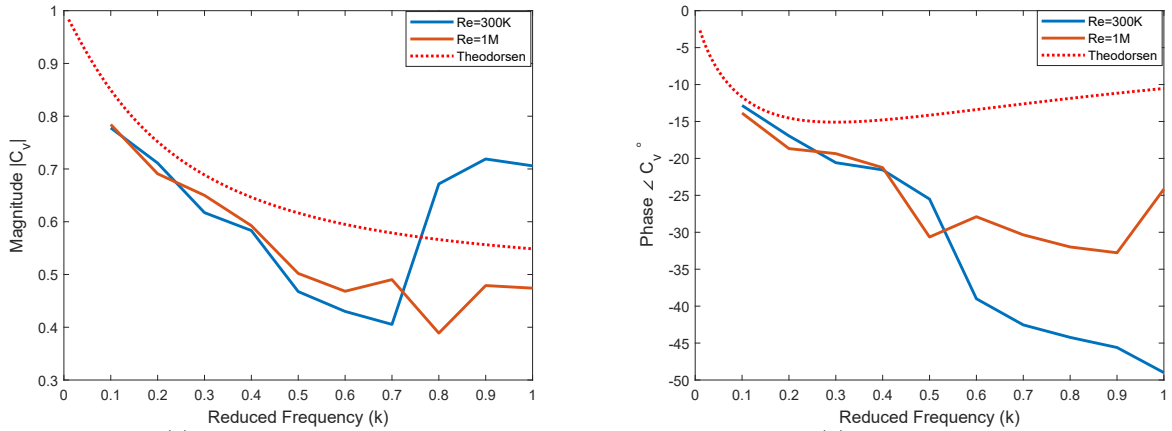

(a) Magnitude Variation. (b) Phase Variation.

Figure 11: Computational results of the frequency responses of the unsteady, viscous, circulatory lift coefficient C_{L_C} at different Reynolds numbers.

V. Conclusion

In this paper, we developed a theoretical unsteady viscous aerodynamic model for an oscillating thin airfoil with arbitrary time-varying camber. The model is based on the unsteady triple deck theory; a boundary layer theory that accounts for the transition at the trailing edge from a Blasius boundary layer to Goldstein wake layer. As such, it accounts for more details near the trailing edge region such as trailing edge stall. Using the developed model, we provided a viscous correction to Theodorsen's potential-flow frequency response function. It is shown that viscosity leads to a significant phase lag at high frequencies and low Reynolds numbers. This phase lag, which is not predicted by Theodorsen's potential-flow model, is expected to affect an instability boundary, hence, it may explain the current weak predictability of flutter boundaries. Computational fluid dynamic simulations solving the incompressible Navier-Stokes equations

are performed using ANSYS FLuent. The computational results corroborate our theoretical predictions. In fact, the computational phase lag is even more exaggerated.

Acknowledgments

The authors would like to acknowledge the NSF grant CMMI-1635673.

References

[1]Prandtl, L., "Über die Entstehung von Wirbeln in der idealen Flüssigkeit, mit Anwendung auf die Tragflügeltheorie und andere Aufgaben," *Vorträge aus dem Gebiete der Hydro-und Aerodynamik (Innsbruck 1922)*, Springer, 1924, pp. 18–33.

[2]Birnbaum, W., "Der Schlagflugelpropeller und die Kleinen Schwingungen elastisch befestigter Tragfluegel." *Z Flugtech Motorluftschiffahrt*, Vol. 15, 1924, pp. 128–134.

[3]Wagner, H., "Uber die entstehung des dynamischen auftriebs von tragflugeln," *ZAMM*, Vol. 5, 1925.

[4]Theodorsen, T., "General Theory of Aerodynamic Instability and the Mechanism of Flutter," Tech. Rep. 496, NACA, 1935.

[5]Von Karman, T. and Sears, W. R., "Airfoil theory for nonuniformmotion." *J. Aeronautical Sciences*, Vol. 5, No. 10, 1938, pp. 379–390.

[6]Jones, M. A., "The separated flow of an inviscid fluid around a moving flat plate," *Journal of Fluid Mechanics*, Vol. 496, 2003, pp. 405–441.

[7]Yongliang, Y., Binggang, T., and Huiyang, M., "An analytic approach to theoretical modeling of highly unsteady viscous flow excited by wing flapping in small insects," *Acta Mechanica Sinica*, Vol. 19, No. 6, 2003, pp. 508–516.

[8]Pullin, D. I. and Wang, Z., "Unsteady forces on an accelerating plate and application to hovering insect flight," *Journal of Fluid Mechanics*, Vol. 509, 2004, pp. 1–21.

[9]Ansari, S. A., Żbikowski, R., and Knowles, K., "Non-linear unsteady aerodynamic model for insect-like flapping wings in the hover. Part 1: methodology and analysis," *Proceedings of the Institution of Mechanical Engineers, Part G: Journal of Aerospace Engineering*, Vol. 220, No. 2, 2006, pp. 61–83.

[10]Michelin, S. and Smith, S. G. L., "An unsteady point vortex method for coupled fluid–solid problems," *Theoretical and Computational Fluid Dynamics*, Vol. 23, No. 2, 2009, pp. 127–153.

[11]Tchieu, A. A. and Leonard, A., "A discrete-vortex model for the arbitrary motion of a thin airfoil with fluidic control," *Journal of Fluids and Structures*, Vol. 27, No. 5, 2011, pp. 680–693.

[12]Wang, C. and Eldredge, J. D., "Low-order phenomenological modeling of leading-edge vortex formation," *Theoretical and Computational Fluid Dynamics*, Vol. 27, No. 5, 2013, pp. 577–598.

[13]Ramesh, K., Gopalarathnam, A., Edwards, J. R., Ol, M. V., and Granlund, K., "An unsteady airfoil theory applied to pitching motions validated against experiment and computation." *Theoretical and Computational Fluid Dynamics*, 2013, pp. 1–22.

[14]Ramesh, K., Gopalarathnam, A., Granlund, K., Ol, M. V., and Edwards, J. R., "Discrete-vortex method with novel shedding criterion for unsteady aerofoil flows with intermittent leading-edge vortex shedding," *Journal of Fluid Mechanics*, Vol. 751, 2014, pp. 500–538.

[15]Yan, Z., Taha, H. E., and Hajj, M. R., "Geometrically-Exact Unsteady Model for Airfoils Undergoing Large Amplitude Maneuvers," *Aerospace Science and Technology*, Vol. 39, 2014, pp. 293–306.

[16]Li, J. and Wu, Z.-N., "Unsteady lift for the Wagner problem in the presence of additional leading/trailing edge vortices," *Journal of Fluid Mechanics*, Vol. 769, 2015, pp. 182–217.

[17]Dickinson, M. H., Lehmann, F.-O., and Sane, S. P., "Wing rotation and the aerodynamic basis of insect flight." *Science*, Vol. 284, No. 5422, 1999, pp. 1954–1960.

[18]Wang, Z. J., Birch, J. M., and Dickinson, M. H., "Unsteady forces in hovering flight: computation vs experiments," *Journal of Experimental Biology*, Vol. 207, 2004, pp. 449–460.

[19]Wang, Z., "Vortex shedding and frequency selection in flapping flight," *Journal of Fluid Mechanics*, Vol. 410, 2000, pp. 323–341.

[20]Ramamurti, R. and Sandberg, W., "A three-dimensional computational study of the aerodynamic mechanisms of insect flight," *Journal of Experimental Biology*, Vol. 205, No. 10, 2002, pp. 15071518.

[21]Sears, W. R., "Unsteady motion of airfoils with boundary-layer separation," *AIAA journal*, Vol. 14, No. 2, 1976, pp. 216–220.

[22]Crighton, D. G., "The Kutta condition in unsteady flow," *Annual Review of Fluid Mechanics*, Vol. 17, No. 1, 1985, pp. 411–445.

[23]Howarth, L., "The theoretical determination of the lift coefficient for a thin elliptic cylinder," *Proceedings of the Royal Society of London. Series A, Mathematical and Physical Sciences*, Vol. 149, No. 868, 1935, pp. 558–586.

[24]Basu, B. C. and Hancock, G. J., "The unsteady motion of a two-dimensional aerofoil in incompressible inviscid flow," *Journal of Fluid Mechanics*, Vol. 87, No. 01, 1978, pp. 159–178.

[25]Daniels, P. G., "On the unsteady Kutta condition," *The Quarterly Journal of Mechanics and Applied Mathematics*, Vol. 31, No. 1, 1978, pp. 49–75.

[26]Satyanarayana, B. and Davis, S., "Experimental studies of unsteady trailing-edge conditions," *AIAA Journal*, Vol. 16, No. 2, 1978, pp. 125–129.

[27]Bass, R. L., Johnson, J. E., and Unruh, J. F., "Correlation of lift and boundary-layer activity on an oscillating lifting surface," *AIAA Journal*, Vol. 20, No. 8, 1982, pp. 1051–1056.

[28]Rott, N. and George, M. B. T., *An Approach to the Flutter Problem in Real Fluids*, Inst. of Aeronautical Sciences, 1955.

[29]Abramson, H. N. and Chu, H.-H., *A discussion of the flutter of submerged hydrofoils*, Southwest Research Institute, 1958.

[30]Henry, C. J., *Hydrofoil Flutter Phenomenon and Airfoil Flutter Theory*, Davidson Laboratory, 1961.

[31]Chu, W.-H., "An aerodynamic analysis for flutter in Oseen-type viscous flow," *Journal of the Aerospace Sciences*, 1962.

[32]Shen, S. F. and Crimi, P., "The theory for an oscillating thin airfoil as derived from the Oseen equations," *Journal of Fluid Mechanics*, Vol. 23, No. 03, 1965, pp. 585–609.

[33]Woolston, D. S. and Castile, G. E., "Some effects of variations in several parameters including fluid density on tbe flutter speed of light uniform cantilever wings," 1951.

[34]Chu, W.-H. and Abramson, H. N., "An Alternative Formulation of the Problem of Flutter in Real Fluids," *Journal of the Aerospace Sciences*, 1959.

[35]Abramson, H. N., Chu, W.-H., and Irick, J. T., "Hydroelasticity with special reference to hydrofoil craft." Tech. rep., DTIC Document, 1967.

[36]Savage, S. B., Newman, B. G., and Wong, D. T.-M., "The role of vortices and unsteady effects during the hovering flight of dragonflies," *The Journal of Experimental Biology*, Vol. 83, No. 1, 1979, pp. 59–77.

[37]Orszag, S. A. and Crow, S. C., "Instability of a Vortex Sheet Leaving a Semi-Infinite Plate," *Studies in Applied Mathematics*, Vol. 49, No. 2, 1970, pp. 167–181.

[38]Ansari, S. A., Zbikowski, R., and Knowles, K., "Non-linear Unsteady Aerodynamic Model for Insect-Like Flapping Wings in the Hover. Part2: Implementation and Validation," *J. of Aerospace Engineering*, Vol. 220, 2006, pp. 169–186.

[39]Pitt Ford, C. W. and Babinsky, H., "Lift and the leading-edge vortex," *Journal of Fluid Mechanics*, Vol. 720, 2013, pp. 280–313.

[40]Graftieaux, L., Michard, M., and Grosjean, N., "Combining PIV, POD and vortex identification algorithms for the study of unsteady turbulent swirling flows," *Measurement Science and Technology*, Vol. 12, No. 9, 2001, pp. 1422.

[41]Hemati, M. S., Eldredge, J. D., and Speyer, J. L., "Improving vortex models via optimal control theory," *Journal of Fluids and Structures*, Vol. 49, 2014, pp. 91–111.

[42]Brown, S. N. and Daniels, P. G., "On the viscous flow about the trailing edge of a rapidly oscillating plate," *Journal of Fluid Mechanics*, Vol. 67, No. 04, 1975, pp. 743–761.

[43]Brown, S. N. and Cheng, H. K., "Correlated unsteady and steady laminar trailing-edge flows," *Journal of Fluid Mechanics*, Vol. 108, 1981, pp. 171–183.

[44]Lighthill, M. J., "On boundary layers and upstream influence. II. Supersonic flows without separation," *Proceedings of the Royal Society of London A: Mathematical, Physical and Engineering Sciences*, Vol. 217, The Royal Society, 1953, pp. 478–507.

[45]Messiter, A. F., "Boundary-layer flow near the trailing edge of a flat plate," *SIAM Journal on Applied Mathematics*, Vol. 18, No. 1, 1970, pp. 241–257.

[46]Stewartson, K., "On the flow near the trailing edge of a flat plate," *Proceedings of the Royal Society of London A: Mathematical, Physical and Engineering Sciences*, Vol. 306, The Royal Society, 1968, pp. 275–290.

[47]Brown, S. N. and Stewartson, K., "Trailing-edge stall," *Journal of Fluid Mechanics*, Vol. 42, No. 03, 1970, pp. 561–584.

[48]Jobe, C. E. and Burggraf, O. R., "The numerical solution of the asymptotic equations of trailing edge flow," *Proceedings of the Royal Society of London A: Mathematical, Physical and Engineering Sciences*, Vol. 340, The Royal Society, 1974, pp. 91–111.

[49]Veldmann, A. E. P. and Van de Vooren, A. I., "Drag of a finite plate," *Proceedings of the Fourth International Conference on Numerical Methods in Fluid Dynamics*, Springer, 1975, pp. 423–430.

[50]Chow, R. and Melnik, R. E., "Numerical solutions of the triple-deck equations for laminar trailing-edge stall," *Proceedings of the Fifth International Conference on Numerical Methods in Fluid Dynamics June 28–July 2, 1976 Twente University, Enschede*, Springer, 1976, pp. 135–144.

[51]Krylov, N. M. and Bogoliubov, N. N., *Introduction to Non-Linear Mechanics.(AM-11)*, Vol. 11, Princeton University Press, 1943.

[52]Schlichting, H. and Truckenbrodt, E., *Aerodynamics of the Airplane*, McGraw-Hill, 1979.

[53]Bisplinghoff, R. L., Ashley, H., and Halfman, R. L., *Aeroelasticity*, Dover Publications, New York, 1996.

[54]Robinson, A. and Laurmann, J. A., *Wing theory*, Cambridge University Press, 1956.

[55]Küssner, H. G., "Schwingungen von Flugzeugflügeln," *Jahrbuch der deutscher Versuchsanstalt für Luftfahrt especially Section E3 Einfluss der Baustoff-Dämpfung*, 1929, pp. 319–320.

[56]Garrick, I. E., "On some reciprocal relations in the theory of nonstationary flows," Tech. Rep. 629, NACA, 1938.

[57]Ogata, K. and Yang, Y., "Modern control engineering," 1970.

[58]Wilcox, D. C. et al., *Turbulence modeling for CFD*, Vol. 2, DCW industries La Canada, CA, 1998.

[59]Menter, F. R., "Two-equation eddy-viscosity turbulence models for engineering applications," *AIAA journal*, Vol. 32, No. 8, 1994, pp. 1598–1605.